RANDOM GENERATION OF COHERENT SPIN WAVE SOLITONS FROM INCOHERENT SPIN WAVES

Carl E. Patton, Mingzhong Wu, and Pavol Krivosik
Department of Physics, Colorado State University
Fort Collins, Colorado, 80523

ABSTRACT

This paper reports on the random generation of coherent envelope solitons from incoherent waves in a medium with an instantaneous nonlinearity, and specifically, in a magnetic thin film strip. One excites a propagating incoherent spin wave packet and observes the random appearance of spin wave envelope solitons from the propagating packet. The random solitons are as coherent as traditional envelope solitons, but both the peak amplitude and timing are random.

1. INTRODUCTION

Spin wave envelope solitons have high potential for microwave signal processing applications. So far, all research on spin wave solitons has involved only coherent waves. In real magnetic thin film systems, however, spin waves with only partial coherence are more common because of, for example, thermal fluctuations.

It has been discovered that incoherent optical spatial solitons could be formed from spatially and temporally incoherent light beams (Mitchell *et al*., 1996; Mitchell *et al*., 1997; Chen *et al*., 1998). For the formation of such incoherent optical solitons, the medium must have a non-instantaneous nonlinearity, that is, a nonlinear response time that is much longer than the timescale for the change of the speckle pattern across the beam. In this situation, the nonlinearity responds to the time averaged spatial envelope of the beam cross section, not to the localized instantaneous speckle regions inside. Very recently, incoherent solitons have also been observed in media with an instantaneous nonlinearity, that is, a nonlinear response time that is much shorter than the correlation time of the incoherent waves (Picozzi *et al*., 2004). In this work, domain-wall type incoherent solitons were formed from two co-propagating incoherent light waves in an optical fiber system.

This paper reports on the formation of spin wave envelope solitons from incoherent spin waves in a thin film magnetic medium with an instantaneous nonlinearity. It is found that if one excites a temporal packet of incoherent spin waves in a magnetic thin film strip, one can observe a fundamentally new type of soliton, a so-called random soliton. Such solitons randomly appear from the propagating spin wave packet, with random peak amplitude, random timing, and a short lifetime. In spite of the incoherent nature of the propagating spin wave packet and the random nature of the soliton generation process, the solitons, when realized, show coherent properties of the sort found for traditional envelope solitons. These results demonstrate the first realization of coherent solitons from incoherent waves.

The experiment utilized nonlinear spin wave pulses propagated in a long and narrow magnetic thin film strip. The experimental configuration was set to allow the propagation of spin waves with attractive or self-focusing nonlinearity and support the formation of bright spin wave envelope solitons. One first uses a pulse of broadband microwave noise to excite an incoherent spin wave packet at one end of the film strip. One then can trace the propagation of the wave packet along the film strip. The correlation time of the incoherent spin wave packet is determined by the bandwidth of the spin wave signal. The nonlinear response time of the film is inversely proportional to the power of the signal. When the spin wave amplitude is sufficiently large to push the nonlinear response time below the correlation time, one can realize an instantaneous nonlinear response and observe random spin wave envelope solitons.

2. EXPERIMENT

Figure 1 shows the experimental set-up. The yttrium iron garnet (YIG) magnetic film strip is magnetized to saturation by a static magnetic field parallel to the length of the strip. This film/field configuration supports the propagation of backward volume spin waves (Stancil, 1993; Kabos and Stalmachov, 1994) that have an attractive nonlinearity. Three microstrip transducers are placed over the YIG strip. One is used for excitation and the other two are used for detection, as indicated. The noise source, fast switch, and broadband microwave amplifier provide a well defined noise pulse at some controllable power level. Amplified input noise pulses

Report Documentation Page

Public reporting burden for the collection of information is estimated to average 1 hour per response, including the time for reviewing instructions, searching existing data sources, gathering and maintaining the data needed, and completing and reviewing the collection of information. Send comments regarding this burden estimate or any other aspect of this collection of information, including suggestions for reducing this burden, to Washington Headquarters Services, Directorate for Information Operations and Reports, 1215 Jefferson Davis Highway, Suite 1204, Arlington VA 22202-4302. Respondents should be aware that notwithstanding any other provision of law, no person shall be subject to a penalty for failing to comply with a collection of information if it does not display a currently valid OMB control number.

1. REPORT DATE	2. REPORT TYPE	3. DATES COVERED
01 NOV 2006	**N/A**	**-**

4. TITLE AND SUBTITLE	5a. CONTRACT NUMBER
Random Generation Of Coherent Spin Wave Solitons From Incoherent Spin Waves	5b. GRANT NUMBER
	5c. PROGRAM ELEMENT NUMBER
6. AUTHOR(S)	5d. PROJECT NUMBER
	5e. TASK NUMBER
	5f. WORK UNIT NUMBER

7. PERFORMING ORGANIZATION NAME(S) AND ADDRESS(ES)	8. PERFORMING ORGANIZATION REPORT NUMBER
Department of Physics, Colorado State University Fort Collins, Colorado, 80523	

9. SPONSORING/MONITORING AGENCY NAME(S) AND ADDRESS(ES)	10. SPONSOR/MONITOR'S ACRONYM(S)
	11. SPONSOR/MONITOR'S REPORT NUMBER(S)

12. DISTRIBUTION/AVAILABILITY STATEMENT
Approved for public release, distribution unlimited

13. SUPPLEMENTARY NOTES
See also ADM002075.

14. ABSTRACT

15. SUBJECT TERMS

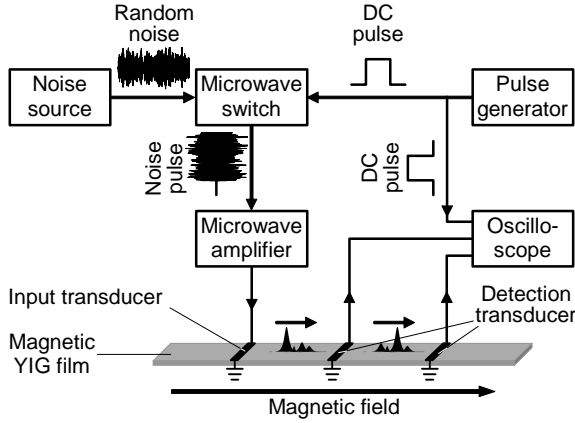| 16. SECURITY CLASSIFICATION OF:			17. LIMITATION OF ABSTRACT	18. NUMBER OF PAGES	19a. NAME OF RESPONSIBLE PERSON
a. REPORT **unclassified**	b. ABSTRACT **unclassified**	c. THIS PAGE **unclassified**	**UU**	**5**	

Fig. 1. Schematic of the experimental arrangement based on a magnetic yttrium iron garnet (YIG) film strip.

excite incoherent propagating spin wave packets in the film strip. The detected propagating spin wave signals are analyzed with a broadband real time microwave oscilloscope.

For the data below, the YIG film strip was 6.8 μm thick, 2.2 mm wide, and 46 mm long. It was cut from a larger single crystal YIG film grown on a gadolinium gallium garnet substrate by standard liquid phase epitaxy technique. The film had unpinned surface spins and a narrow ferromagnetic resonance linewidth. The static magnetic field was set at 1368 Oe. The microstrip transducers were 50 μm wide and 2 mm long. The detection transducers were held at displacements (x) of 5.3 mm and 10.6 mm from the input transducer. The input noise pulses had a maximum power level of 5 W, durations of several tens of nanoseconds, and a repetition rate of 6 kHz. The short pulse duration and low repetition rate served to ensure that there were no heating effects in the film.
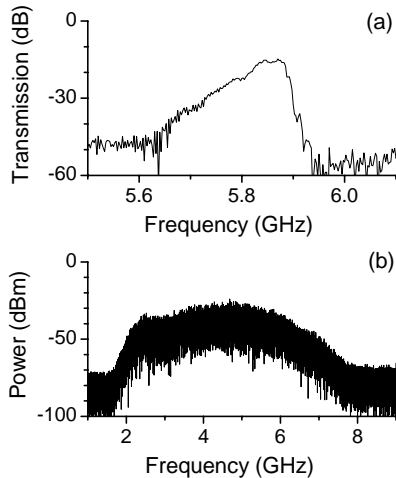

Fig. 2. (a) Transmission loss versus frequency response for the YIG film/transducer structure. (b) Power frequency spectrum for the noise signal.

Figure 2 (a) shows the low-power transmission versus frequency response of the YIG film/transducer structure. The profile shows a spin wave passband from about 5.7 GHz to about 5.9 GHz. Figure 2 (b) shows the power frequency spectrum for the original noise signal. The spectrum shows a noise band from about 2 GHz to about 7 GHz. This is much wider than the spin wave passband. The noise input bandwidth is adequate, therefore, to excite spin waves over the full spectrum of available modes.

3. RESULTS AND DISCUSSION

The main results are shown in Figs. 3 and 4. Figure 3 demonstrates the random nature of the observed solitons. Figure 4 shows selected characteristics of the soliton pulses. Graph pairs (a) – (c) in Fig. 3 show three sets of output power profiles sampled for three different input noise pulses, each with a duration of 50 ns and a power level of about 5 W. In each graph pair, the left and right graphs show single shot oscillograms at the $x = 5.3$ mm and $x = 10.6$ mm detection positions, as indicated. The shadings show the time windows over which there is *bona fide* spin wave signal power at the detection point. On an expanded vertical scale, these regions are distinct. The labels A, B, and C serve to identify the pulses that are solitons.

Figure 3 shows three key results. First, one can see that the input incoherent spin wave packet disperses significantly during its propagation along the film strip.
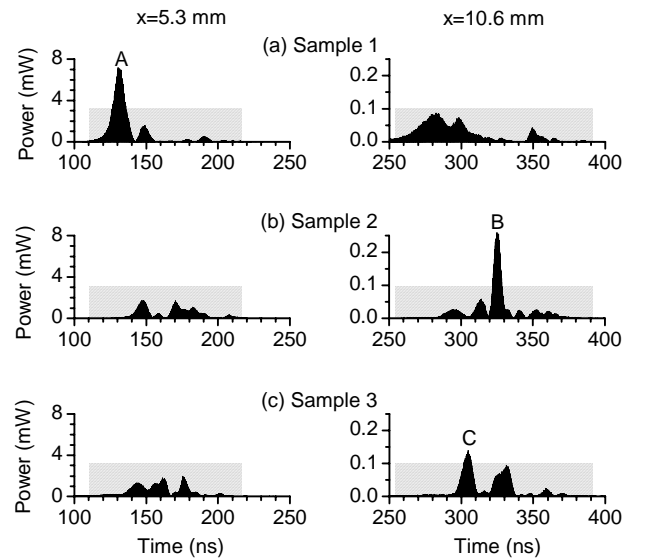

Fig. 3. Graph pairs (a) – (c) show three sets of output power profiles sampled for three different input noise pulses, each with a duration of 50 ns and a power level of about 5 W. The left and right graphs show single shot signals at the two different detection positions, as indicated. The shadings show the time windows for detectable spin wave signals. The A, B, and C labels identify the pulses that are solitons.

The overall signal time windows for the full signal response at $x = 5.3$ mm and $x = 10.6$ mm, as shown by the shadings, are about 105 ns and 138 ns, respectively. These windows are all much wider than the initial input pulse width of 50 ns.

Second, one can see that for a given input noise pulse, the solitons that are realized appear randomly. In Sample 1, for example, one sees a leading soliton (labeled A) at $x = 5.3$ mm but no solitons at $x = 10.6$ mm. For Sample 2, in contrast, there are no solitons at $x = 5.3$ mm, while at $x = 10.6$ mm, one finds a soliton (labeled B) in the middle of the signal time window. In Sample 3, there are several weak pulses but no solitons at $x = 5.3$ mm, while the trace for $x = 10.6$ mm shows a leading soliton pulse (labeled C) and a follow-on non-soliton pulse.

Third, the overall signal time window power profile and the appearance of solitons are *completely random* from sample to sample. If the measurements are extended to more nominally identical input noise pulses, each one gives a totally different response.

Figure 4 shows details on the soliton characteristics of pulse A in graph (a) of Fig. 3. Graph (a) shows the measured power profile (gray shading) on an expanded time scale and a hyperbolic secant squared functional fit to these data (black curve). Graphs (b) and (c) show the corresponding relative phase profile and frequency spectrum for the pulse, respectively. The phase change in graph (b) is measured relative to a reference cw signal (Nash *et al.*, 1998). The frequency spectrum is obtained through a fast Fourier transform analysis of the signal pulse. Graph (d) shows the transmission coefficient
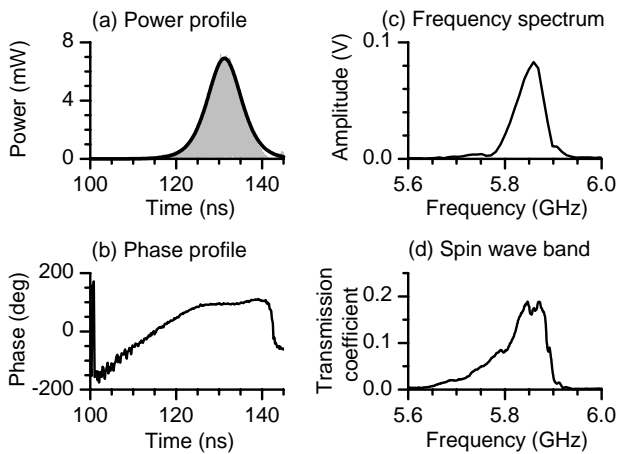

Fig. 4. Expanded time view of pulse A in Fig. 3 (a), along with phase and frequency characteristics. (a) Measured power profile (gray shading) and a fit to a hyperbolic secant squared function (black curve). (b) Relative phase versus time profile. (c) Frequency spectrum. (d) Transmission coefficient versus frequency response of the YIG film/transducer structure.

versus frequency response of the YIG film/transducer structure. This is the same as in Fig. 2 (a), but with a linear vertical scale. This response serves as a basis of comparison between the soliton frequency spectrum and the spin wave passband.

Figure 4 provides evidence that pulse A constitutes a spin wave envelope soliton. Graph (a) shows that the envelope of the pulse can be nicely fitted to the hyperbolic secant form expected for envelope solitons (Ablowitz and Segur, 1985; Kivshar and Agrawal, 2003). Graph (b) shows that the phase of the pulse is constant across the central portion of the pulse, another key soliton property (Kalinikos *et al.*, 1997; Nash *et al.*, 1998). Graphs (c) and (d) show that the frequency spectrum of the pulse matches closely to the spin wave passband for the YIG strip. This match up indicates that the soliton formation involves modes over the entire spin wave passband. This is in contrast with traditional envelope solitons that are formed with single frequency input pulses. Moreover, both the phase profile and the frequency spectrum appear very smooth, clean, and noise free. These data show that one can use a wide band noise input to produce envelope solitons that are as coherent and well behaved as traditional envelope solitons. This is a fourth key result. Pulses B and C in Fig. 3 have the same soliton characteristics as pulse A.

The data in Figs. 3 and 4 demonstrate the generation of coherent solitons from incoherent waves and the random nature of the generation process. The physical process for such soliton generation may be described as follows. First, the propagating incoherent spin wave packet consists of a range of uncorrelated spin wave modes. Second, at different times along the propagation path, these uncorrelated modes experience different degrees of constructive interactions that lead to the formation of strong or weak localized spin wave pulses. Third, for the strong pulses, one has a nonlinear response time T_n of the YIG film that is shorter than the correlation time T_c of the spin wave modes and the pulse can evolve into a soliton quickly. Once realized, the soliton is coherent over a time interval that is shorter than the correlation time.

The nonlinear response time T_n and the correlation time T_c can be estimated through the relations $N|u|^2 T_n = \phi_d$ and $T_c = 1/\Delta f$, respectively, where N is a nonlinearity coefficient, $|u|^2$ represents the spin wave power, ϕ_d is the dispersion-induced phase shift across the pulse width, and Δf is the half-power width of the spin wave passband. Information on the nonlinear response of spin waves and the definitions of the corresponding parameters are given in references (Chen *et al.*, 1994; Slavin *et al.*, 1994; Nash *et al.*, 1998). For the situation in Figs. 3 and 4, the nonlinear response time and the
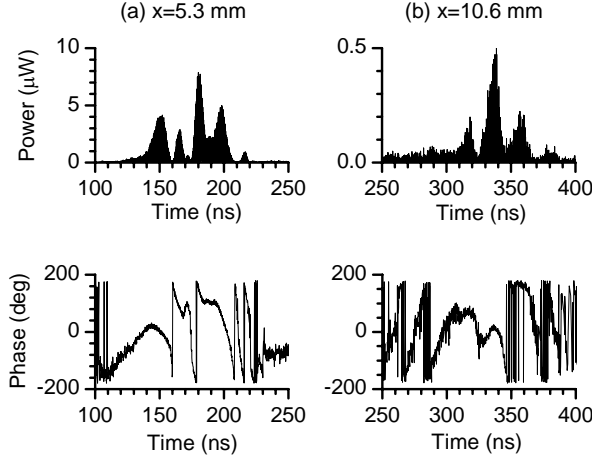
Fig. 5. Output power profiles and relative phase profiles for a 50 ns wide input noise pulse with a power level of about 0.2 mW. The left and right graphs are for two different detection positions, as indicated.

correlation time are estimated to be $T_n \approx$ 1-5 ns and $T_c \approx$ 17 ns, respectively. These times are consistent with the scenario given above.

One simple test of the $T_n < T_c$ soliton formation hypothesis is to reduce the input power. For weak spin wave pulses, the nonlinear response time T_n is relatively long and the pulses cannot acquire enough nonlinear phase shift to develop into solitons within the correlation time T_c. Figure 5 shows single shot output signals for an input noise pulse at a low power level of about 0.2 mW. The other conditions were the same as for the data in Figs. 3 and 4. The upper and lower graphs show power profiles and relative phase profiles, respectively. The power versus time profiles in Fig. 5 are somewhat similar to those in Fig. 3. These data demonstrate the random nature of the spin wave pulse formation process, even for low power signals.

However, the phase data in Fig. 5 are in stark contrast with the corresponding high power data in Fig. 4 (b). For a low power noise pulse input, the phase profiles of the random spin wave pulses are all concave downward, just as one would expect for linear spin wave pulses with positive dispersion (Nash *et al.*, 1998). These low-power data indicate that a short nonlinear response time and an instantaneous nonlinearity are required for the formation of coherent solitons from incoherent waves.

Turn now to the random nature of the soliton generation process. One explanation for this randomness lies in the fact that the correlation time T_c of the spin wave modes is much shorter than the temporal width T_p of the overall spin wave packet. For the situation in Figs. 3 and 4, the time window T_p is in the 100 - 140 ns range.
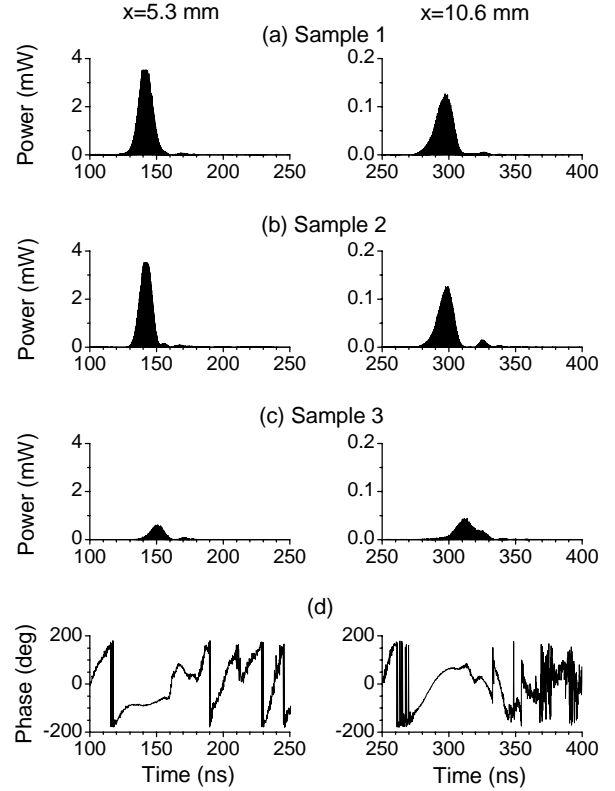

Fig. 6. Graph pairs (a) – (c) show three sets of output power profiles sampled for three separate input noise pulses. The input pulses had a duration of 10 ns and a power level of about 5 W. The left and right graphs show single shot signals at the two different detection positions, as indicated. Graph pair (d) show the relative phase versus time profiles for the signals shown in graph pair (a).

When the condition $T_c < T_p$ is satisfied, the spin wave modes randomly change their phase and, hence, interact with each other randomly on any time scale greater than the relatively short correlation time. This leads to the random nature of the observed soliton generation, both spatially and temporally.

The above scenario may be tested through the use of short input noise pulses. In this case, the condition $T_c > T_p$ will apply, and one should produce quasi-coherent spin wave packets. One will then have stable interactions between the spin wave modes. The realized solitons will then have more-or-less traditional envelope soliton characteristics. This expectation was tested through a repeat of the Fig. 3 and Fig. 4 experiments, but with 10 ns wide input noise pulses.

Figure 6 shows the experimental data for narrow input noise pulses. The format is the same as for Fig. 3. From top to bottom, one sees that single shot data for three nominally identical input pulses give different signals. The pulses in graphs (a) and (b) are solitons,

while the pulses in graph (c) are not. The constant phase profiles in graph (d) clearly demonstrate the soliton nature of the corresponding pulses in graph (a). As in Fig. 2, one sometimes obtains a soliton and sometimes not. From left to right, however, one sees that for a given input pulse, the signals at different positions are more-or-less the same. This means that, when realized, the solitons can be tracked from one observation point to another. These data support the thesis that short correlation times relative to the packet width are needed in order to obtain random solitons.

CONCLUSIONS

In conclusion, this paper reports the random generation of temporal envelope solitons from incoherent waves. The realized solitons are as coherent as traditional envelope solitons, but both the peak amplitude and timing are random. For the formation of such random solitons, it is necessary that nonlinear response time be shorter than the correlation time of the incoherent wave packets, and that the correlation time be shorter than the width of the wave packets. This type of random soliton phenomena should be common to a wide range of nonlinear dispersive soliton supporting systems.

ACKNOWLEDGMENTS

REFERENCES

Ablowitz, M. J. and Segur, H., 1985: *Solitons and the Inverse Scattering Transform* (SIAM, Philadelphia).

Chen, M., Tsankov, M. A., Nash, J. M., and Patton, C. E., 1994: Backward-volume-wave Microwave-envelope Solitons in Yttrium Iron Garnet Films, *Phys. Rev. B*, **49**, 12773-12790.

Chen, Z. G., Mitchell, M., Segev, M., Coskun, T. H., and Christodoulides, D. N., 1998: Self-Trapping of Dark Incoherent Light Beams, *Science*, **280**, 889-892.

Kabos, P. and Stalmachov, V. S., 1994: *Magnetostatic Waves and Their Applications* (Chapman & Hall, London).

Kalinikos, B. A., Kovshikov, N. G., and Patton, C. E., 1997: Decay Free Microwave Magnetic Envelope Soliton Pulse Trains in Yttrium Iron Garnet Thin Films, *Phys. Rev. Lett.*, **78**, 2827-2830.

Kivshar, Y. S. and Agrawal, G. P., 2003: *Optical Solitons* (Academic, San Diego).

Mitchell, M., Chen, Z. G., Shih, M. F., and Segev, M., 1996: Self-Trapping of Partially Spatially Incoherent Light, *Phys. Rev. Lett.*, **77**, 490-493.

Mitchell, M. and Segev, M., 1997: Self-trapping of incoherent white light, *Nature*, **387**, 880-883.

Nash, J. M., Kabos, P., Staudinger, R., and Patton, C. E., 1998: Phase Profiles of Microwave Magnetic Envelope Solitons, *J. Appl. Phys.*, **83**, 2689-2699.

Picozzi, A., Haelterman, M., Pitois, S., and Millot, G., 2004: Incoherent Solitons in Instantaneous Response Nonlinear Media, *Phys. Rev. Lett.*, **92**, 143906 1-4.

Slavin, A. N., Kalinikos, B. A., and Kovshikov, N. G., 1994: *Nonlinear Phenomena and Chaos in Magnetic Materials*, edited by P. E. Wigen (World Scientific, Singapore), Chap. 9.

Stancil, D. D., 1993: *Theory of magnetostatic waves* (Springer-Verlag, New York).